ENHANCEMENT OF IONIZATION RATES FORMULAS IN TUNNELING AND BARRIER-SUPPRESSION REGIMES

Jasna Stevanović[1], Violeta Petrović[1], Hristina Delibašić-Marković[1], Ivan Petrović[2]

[1]University of Kragujevac, Faculty of Science, Radoja Domanovića 12, 34000 Kragujevac, Serbia, jasna.stevanovic@pmf.kg.ac.rs, violeta.petrovickg@gmail.com, hristina.delibasic@pmf.kg.ac.rs

[2]Academy of Professional Studies Šumadija, Department in Kragujevac, Kosovska 8, 34000 Kragujevac, Serbia, kgivanpetrovic@gmail.com

ORIGINAL SCIENTIFIC PAPER

Received: 14 July 2026.
Accepted: 21 September 2026.
Published: 16 November 2026.
DOI: https://doi.org/10.63395/STEDConf15022026139S473

Corresponding Author: Jasna Stevanović, University of Kragujevac, Faculty of Science, Radoja Domanovića 12, 34000 Kragujevac, Serbia, jasna.stevanovic@pmf.kg.ac.rs

Copyright © 2026 Jasna Stevanović et al.; published by UNIVERSITY PIM. This work licensed under the Creative Commons Attribution-NonCommercial-NoDerivs 4.

Citation: Stevanović, J. et al. (2026). Enhancement of Ionization Rates Formulas in Tunneling and Barrier-Suppression Regimes. In Kojić, D. & Sredić. D. (eds.) *Conference proceedings, XV International Conference on Social and Technological Development: STED 2026* (pp. 473-482). Trebinje, B&H: University PIM.

ABSTRACT

The precise modelling of laser–target interactions in the regimes of tunneling and barrier-suppression ionizations is important, as these mechanisms dominate in the strong-field regime. In this study, we examine the dynamics of the transition from tunneling to barrier-suppression ionization by applying an empirically adapted formula. Within an enhanced analytical framework, the shift between these two ionization regimes is characterized more clearly. The proposed model preserves the computational efficiency of analytical approaches by improving their physical consistency. While it is generally accepted that the ionization rate depends on the intensity of the applied laser field, our findings indicate that it is also influenced by the initial momentum of the outgoing electron, as well as by the laser frequency. We further demonstrate that, in addition to long-range Coulomb interactions, these effects play a significant role in the strong-field ionization domain, providing a basis for exploring new mechanisms in intense laser–matter interactions.

Keywords: strong-field ionization, laser intensity, initial momentum, Coulomb interactions

INTRODUCTION

The continuous development of laser technology, along with experimental and theoretical advancements, has greatly enhanced our understanding of light-matter interactions. The newfound availability of laser pulses with high intensity and short duration has opened avenues for studying atomic and molecular dynamics on their natural time scales. The electronic configuration of atoms and molecules can be significantly altered by intense laser fields, leading to nonlinear dynamics that lie beyond the scope of perturbation theory [1], [2], [3]. Laser-induced ionization is one of the

fundamental processes in modern strong-field physics and has been the subject of extensive theoretical and experimental investigations over the past several decades [4]. Depending on the intensity of the applied laser field and its frequency, different ionization mechanisms can dominate. The multiphoton ionization regime (MPI) is characterized by the absorption of several photons whose cumulative energy is sufficient to overcome the ionization potential of the target. As the laser intensity increases, the electric field of the laser significantly distorts the Coulomb potential experienced by the bound electron, leading to the tunneling ionization regime (TI). In this process, the electron escapes by quantum-mechanical tunneling through the field-lowered potential barrier, even when the photon energy alone is insufficient to overcome the binding energy [5], [6], [7], [8]. For even stronger laser fields, the Coulomb barrier can be suppressed below the energy level of the bound electron, enabling direct electron escape without tunneling. This mechanism, known as barrier-suppression ionization (BSI) represents the extreme limit of strong-field ionization [9], [10], [11].

The distinction between multiphoton and tunneling ionization regimes is commonly characterized by the Keldysh parameter γ, which provides a measure of the relative importance of photon absorption and tunneling dynamics [5]. In atomic units ($e = \hbar = m_e = 1$, used throughout this paper), parameter γ can be calculated as $\gamma = \frac{\omega\sqrt{2I_p}}{F}$, where ω is laser frequency, I_p is ionization potential and F is the laser electric field strength. For $\gamma < 1$ TI is dominant process, whereas for $\gamma > 1$ leading target ionization is through the MPI mechanism. For $\gamma \sim 1$ there is intermediate regime in which both processes can occur [10].

Understanding electron dynamics in intense laser fields requires accurate modelling of tunneling and barrier-suppression ionization expressions. Such modeling seems to be the first step toward understanding almost all strong-field phenomena When an electron exits the parent atom, its initial momentum distribution and the residual ionic core's influence are all factors that must be considered. These initial conditions have a significant impact on the electron motion caused by the laser field, which in turn impacts the observable features of numerous nonlinear processes. During the tunneling regime, the electron emerges from the Coulomb barrier distorted by lasers with quantum-mechanical characteristics that convey information about both the atomic structure and ionization dynamics. The behavior of ionization rates, photoelectron spectra, and angular distributions however differs in the barrier-suppression regime, where the potential barrier is lowered to allow electrons to escape directly. Therefore, the accurate representation of ionization rates and electron emission characteristics across various laser parameters requires knowledge of the transition between the TI and the BSI regimes. Also, high-order harmonic generation and laser-induced electron diffraction are largely dependent on the conditions prevailing during the ionization step, which also determine the recollision dynamics of the ionized electron with its parent ion [2], [3], [12]. Hence, it is essential to have an in-depth understanding of the dynamics of ionization for both interpretations on experimental measurements and attosecond techniques for studying ultrafast electronic motion on its natural timescale [2].

In this paper, we enhance the analytical description of laser-induced ionization in intense laser fields, combining a modified semi-empirical ionization model with an improved treatment of strong-field electron dynamics. Our approach incorporates physical effects that become significant in the TI and the BSI regimes. The paper is organized as follows: in the next section, we concisely describe the modifications to the ionization rate formulae that account for the non-zero initial momentum of the outgoing electron, the laser frequency and the long-range Coulomb interaction. We then present and discuss our results, followed by a brief conclusion.

ANALYTICAL FRAMEWORK

The theoretical approach developed in this work is based on a modified analytical description of strong-field ionization that extends the semi-empirical ionization model proposed by Tong and Lin [13]. While the original formulation provides an accurate representation of ionization rates for atoms exposed to intense laser fields, it does not explicitly account for the influence of the initial momentum of the outgoing electron, the laser frequency or the continuous dependence on the

ionization regime characterized by the Keldysh parameter γ. To overcome these limitations, new analytical expressions are obtained that incorporate these effects within a unified framework.

The derivation begins with the Tong and Lin ionization formula, which serves as the reference expression for the field-dependent ionization rate in this work [13]. Their work extends the well-known analytical expression for the TI rate to the BSI regime, while maintaining the relative simplicity of the approach:

$$W_{BSI}^{TL}(F) = W_{TI}(F) \times W_{corr}^{TL}(F) \qquad (1)$$

$$W_{corr}^{TL}(F) = \exp\left[-\alpha \frac{Z_c^2}{I_p} \frac{F}{k^3}\right] \qquad (2)$$

Term $W_{TI}(F)$ represents formula for the tunneling ionization rate in intense laser fields based on the Ammosov–Delone–Krainov (ADK) theory [6], [7], [8]. The ADK model assumes a quasistatic electric field, making it valid when the laser field varies slowly compared to the electron tunneling time.

$W_{corr}^{TL}(F)$ is an empirical correction factor expressed in terms of scaled field strength F and scaled ionization energy I_p, with an empirical parameter α, Z_c is the charge seen by the active electron and $k = \sqrt{2I_p}$. Numerical values for empirical parameter α and Z_c are listed in [13], for specific atoms and atomic ions.

The original Tong and Lin formulation is first generalized by introducing the non-zero initial momentum of the outgoing photoelectron, (p), as an explicit variable rather than assuming electron emission with vanishing momentum at the tunnel exit [14]. This modification allows the ionization rate to depend directly on the initial momentum distribution, thereby providing a more realistic description of the electron immediately after ionization. The resulting analytical expression preserves the simplicity of the original model while extending its applicability to realistic situations in which the finite photoelectron momentum acquired during the ionization process cannot be neglected. A second extension concerns the explicit inclusion of laser frequency ω and the Keldysh parameter γ. Consequently, the analytical expression remains valid across the various laser frequency and naturally reproduce the corresponding limiting behaviors through Keldysh parameter γ. Also, we assumed that the angular momentum and magnetic quantum numbers of the valence electrons are zero (l=0, m = 0) in pre-exponential part of $W_{TI}(F)$. Taking all abovementioned into account, the new ionization rate formula is therefore expressed as a function of the laser field strength, the initial photoelectron momentum and laser frequency:

$$W_{BSI}^{TLp}(F,\omega,p) = \frac{C_l^2}{\frac{Zc}{2(2I_p)^{\sqrt{2I_p}-1}}} \left(\frac{2Z^3}{Fn^{*3}}\right)^{\frac{2Zc}{\sqrt{2I_p}}-1} \times \exp\left[-\alpha \frac{Z_c^2}{I_p} \frac{F}{(\sqrt{2I_p})^3}\right] \times \exp\left[-\frac{2Z^3}{3Fn^{*3}} - -\frac{p^2\gamma^3}{3\omega}\right] \qquad (3)$$

In above equation, n^* is effective principal quantum number, Z is charge state of atoms and C_l is coefficient that measures the amplitude of the electron wavefunction in the tunnelling region [13]. Through previous definition of parameter γ, the effects of the laser frequency and the atomic ionization potential are simultaneously incorporated into the improved analytical model. According to the well-established procedure described in [15] it is convenient to use the parabolic coordinates to express initial photoelectron momentum as:

$$p = \frac{1}{2}\left(\sqrt{F\eta - 1} - \frac{1}{\eta\sqrt{F\eta - 1}}\right) \qquad (4)$$

where η is the parabolic coordinate that satisfies the following condition $\eta > 1/F$ [16].

With the parameters p, ω and γ introduced above, we further explore their influence on the ionization rate profile. The dependence of the ionization rate on p describes the momentum-

resolved features of the ionization process, while the dependence on frequency allows the investigation of ionization over a wide range of laser wavelengths. The dependence on γ parameter allows us to verify the corresponding ionization regime. Together, they provide a more complete analytical description of strong-field ionization than the original Tong and Lin formulation.

It is known that Coulomb correction models upgrade the common TI and BSI frameworks by incorporating the long-range Coulomb interaction between the escaping electron and the parent ion [7], [8], [9]. Consequently, despite the increase in laser field intensity, the contribution of the atomic potential remains non-negligible. The inclusion of Coulomb corrections alters the imaginary part of the action, thereby influencing the resulting total ionization rate [7], [8]. Thus, we have upgraded the $\mathrm{W}_{\mathrm{BSI}}^{\mathrm{TLp}}(F,\omega,p)$ formula by incorporating a more general form of the Coulomb interaction [17]:

$$C_{corr}=\left[\frac{(1-\varepsilon)F}{2\frac{Z}{n^{*2}}^{3}}\right]^{-2n^{*}} \qquad (5)$$

The derivation details are given in [17], while parameter ε represents the degree of polarization of the laser field. Therefore, modified ionization rate $\mathrm{W}_{\mathrm{BSI}_{\mathrm{mod}}}^{\mathrm{TL}}(F,\omega,p)$ is expressed as:

$$\mathrm{W}_{\mathrm{BSI}_{\mathrm{mod}}}^{\mathrm{TL}}(F,\omega,p)=\frac{C_l^2}{2(2I_p)^{\frac{Zc}{\sqrt{2I_p}}-1}}\left[\frac{(1-\varepsilon)F}{2\frac{Z}{n^{*2}}^{3}}\right]^{-2n^{*}}\times\exp\left[-\alpha\frac{Z_c^2}{I_p}\frac{F}{(\sqrt{2I_p})^3}\right]\times\exp\left[-\frac{2Z^3}{3Fn^{*2}}-\frac{p^2\gamma^2}{3\omega}\right] \qquad (6)$$

The resulting analytical model preserves the computational efficiency characteristic of semi-analytical approaches while improving their physical consistency. In particular, the derived expression in Eq. (3) accounts for improvements arising from non-zero initial electron momentum and the continuous evolution between the TI and BSI ionization regimes, enabling more accurate predictions of ionization rates and electron dynamics over a broad range of laser parameters. In addition, the influence of the generalized long-range Coulomb potential, given in Eq. (5), on the ionization dynamics is taken into account through Eq. (6).

This framework provides a convenient basis for comparison with numerical simulations and experimental measurements, while maintaining the transparency of an analytical formulation. In the next section, we will compare ionization rates $\mathrm{W}_{\mathrm{BSI}}^{\mathrm{TLp}}(F,\omega,p)$ and $\mathrm{W}_{\mathrm{BSI}_{\mathrm{mod}}}^{\mathrm{TL}}(F,\omega,p)$ for representative atoms, following avaliable numerical data for α, C_l, Z_c in [13], [18].

RESULTS

This section presents the results obtained from the application of the ionization rate formulas given in Eqs. (3) and (6), considering the case of a linearly polarized laser field ($\varepsilon = 0$). Linear polarization represents one of the most extensively studied configurations in strong-field atomic physics because of its relative simplicity and its direct relevance to a wide range of experimental investigations [9], [19], [20].

The analysis focuses on the dependence of the ionization rate on the laser parameters, such as the electric field strength, laser intensity, and frequency, as well as on the atomic properties of the target species (I_p, C_l, α). The predictions obtained from Eqs. (3) and (6) are compared over a broad range of field parameters to evaluate the consistency of the proposed analytical model and to identify the conditions under which their results converge or significantly differ.

Helium and argon atoms are chosen as representative noble gas atoms because they are among the most widely used noble gases in experimental research. Helium is characterized by its simple electronic structure and high ionization potential $I_p^{\mathrm{He}} = 24.59\ \mathrm{eV} = 0.904\ \mathrm{a.u.}$, making it an ideal model system for studying fundamental atomic interactions and collision processes. Argon, in contrast, has a more complex electronic configuration, lower ionization potential,

$I_p^{\mathrm{Ar}} = 15.76\ \mathrm{eV} = 0.579\ \mathrm{a.u.}$ and is widely employed in plasma physics, gas discharge experiments, laser technologies, and spectroscopy due to its favorable physical and chemical properties. Consequently, these two noble gas atoms serve as representative benchmark systems for both experimental and theoretical investigations in atomic and molecular physics [20], [21], [22], [23].

Our study is based on the Ti: sapphire laser system with following parameters: wavelength $\lambda_1 = 800\ \mathrm{nm}$ and frequency $\omega_1 = 0.05696\ \mathrm{a.u.}$,wavelength $\lambda_2 = 1000\ \mathrm{nm}$ and frequency $\omega_2 = 0.0456\ \mathrm{a.u.}$ Since the laser field is linearly polarized, its strength is given by:

$$F_{\mathrm{lin}} = \frac{27.5}{5.1\times10^{9}}\sqrt{I},$$

where I is the intensity of the laser field being used.

As an initial step, the values of the γ parameter for two laser frequences (ω_1, ω_2) are shown for each atom individually (Fig. 1a and Fig. 1b) to verify that the system remains within the TI and the BSI regime ($\gamma < 1$).

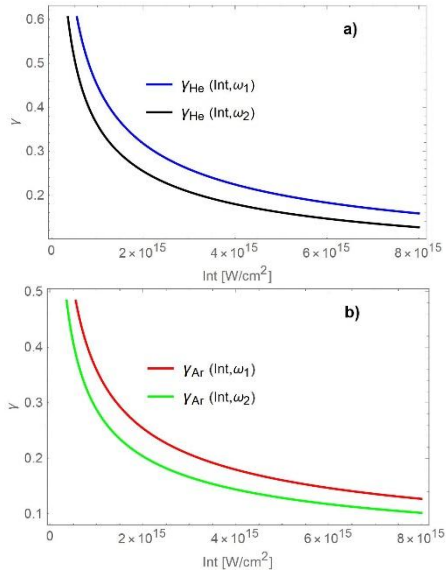


Figure 1. γ parameter for: a) helium atoms, b) argon atoms, for both atoms the intensity is in the range 10^{14} – $8\times10^{15}\ \mathrm{W/cm^2}$

Next, we investigate the influence of the non-zero initial momentum of the outgoing electron and the laser frequency (wavelength) on the ionization rate $\mathrm{W}_{\mathrm{BSI}}^{\mathrm{TLp}}(F,\omega,p)$. The role of the initial momentum is analyzed for different values of the parameter η, allowing us to assess its contribution to the ionization dynamics. The results obtained for helium atoms are presented in Fig. 2, while the corresponding results for argon atoms are shown in Fig. 3.

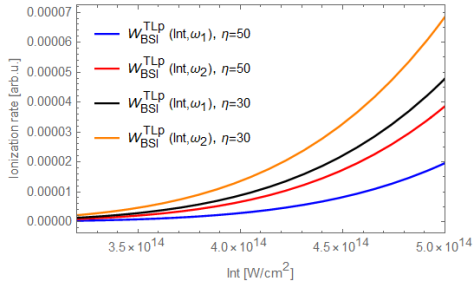


Figure 2. Comparison of the W_{BSI}^{TLp} ionization rates for He atoms, for different η values. The central wavelengths of the laser are $\lambda_1 = 800\ nm$ and $\lambda_2 = 1000\ nm$, $C_l = 2.67, \alpha = 7$ and intensity range is 3.2 x10^{14} - 5x10^{14} W/cm^2

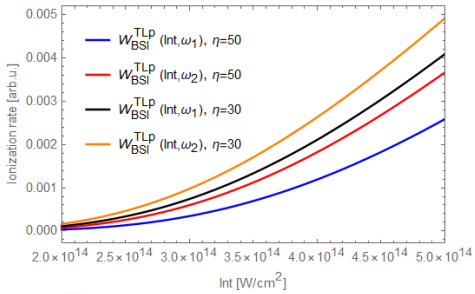


Figure 3. Comparison of the W_{BSI}^{TLp} ionization rates for Ar atoms, for different η values. The central wavelengths of the laser are $\lambda_1 = 800\ nm$ and $\lambda_2 = 1000\ nm$, $C_l = 2.19, \alpha = 9$ and intensity range is 2x10^{14}-5x10^{14} W/cm^2

As a final assessment, the ionization rates $W_{BSI}^{TLp}(F, \omega, p)$ and $W_{BSI_{mod}}^{TL}(F, \omega, p)$ for helium and argon atoms are evaluated to emphasize the influence of the long-range Coulomb potential on the ionization dynamics, see Figs. 4 and 5.

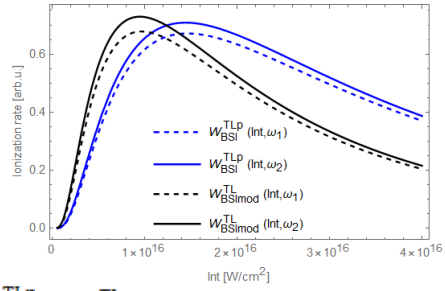


Figure 4. Comparison of the $W_{BSI}^{TLp}$and W_{BSImod}^{TL} ionization rates for He atoms, $\eta = 30, C_l = 2.67, \alpha = 7$. The central wavelengths of the laser are $\lambda_1 = 800\ nm$ and $\lambda_2 = 1000\ nm$, and intensity range is 10^{14} - 10^{16} W/cm^2

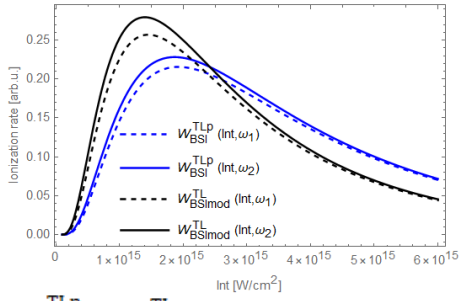


Figure 5. Comparison of the the W_{BSI}^{TLp} and W_{BSImod}^{TL} ionization rates for Ar atoms, $\eta = 30, C_l = 2.19, \alpha = 9$. The central wavelengths of the laser are $\lambda_1 = 800\ nm$ and $\lambda_2 = 1000\ nm$, and intensity range is 10^{14}-10^{16} W/cm^2

The obtained results are presented to assess the validity and accuracy of the analytical model and the proposed analytical expressions. A comprehensive discussion of the results is presented in the subsequent section.

DISCUSSION

The following analysis examines the dependence of the enhanced ionization rates on key laser parameters, including the electric field strength, laser intensity, and frequency, as well as on the intrinsic properties of the target atoms (helium and argon), such as the ionization potential I_p and empirical parameter α. The predictions of Eqs. (3) and (6) are systematically compared over a broad range of field parameters to appraise the consistency of the analytical model and to determine the domains in which these predictions exhibit agreement or significant variance.

The γ parameter values shown in Fig. 1 indicate that the system remains predominantly within the TI and BSI regimes over the investigated parameter range for both atoms. This observation supports the applicability of the employed analytical models and provides the basis for further comparison of the ionization rates. Also, the influence of the non-zero initial momentum of the outgoing electron Eq. (4). and laser frequency on ionization rate is revealed (Fig. 2 and Fig. 3). As the laser intensity increases, the stronger laser field significantly modifies the electron dynamics, resulting in an increased probability of electron excitation and subsequent ionization. This behavior is characteristic of strong-field ionization processes, where the nonlinear interaction between the laser field and the atomic potential plays a dominant role [5], [12]. The variations of parabolic coordinate η and hence the inclusion of the non-zero initial momentum of the outgoing electron, introduce an additional modulation of the ionization response by altering the effective interaction conditions between the laser field and the target system. For specific values of parabolic coordinate η, the ionization rate exhibits a stronger enhancement, indicating that the system parameters can either promote or suppress the electron emission, depending on the degree of coupling to the external field. Furthermore, the influence of the laser frequency becomes significant even at the beginning of the investigated intensity range ~4 x10^{14} $\mathrm{W/cm^2}$. A suitable choice of laser frequency enhances energy transfer from the laser field to the electron, facilitating more efficient population of continuum states and increasing the likelihood of strong-field ionization [24]. Even moderate changes in laser frequency can substantially modify the ionization dynamics for both atoms, see Fig. 2 (orange line) and Fig. 3 (orange line). The combined effect of increasing laser intensity, varying coordinate η, and tuning the laser frequency reveals a significant interplay between laser field strength and system-dependent parameters in the TI and BSI regimes for helium and argon atoms [21], [23].

Additional comparative analyses of the ionization rates $\mathrm{W}_{\mathrm{BSI}}^{\mathrm{TLp}}(F,\omega,p)$ and $\mathrm{W}_{\mathrm{BSI}_{\mathrm{mod}}}^{\mathrm{TL}}(F,\omega,p)$ demonstrate the importance of the long-range Coulomb interaction, as shown in Figs. 4 and 5. The observed increase in the ionization rate can be attributed to the modification of the electron's tunneling pathway by the Coulomb potential. For case of $\mathrm{W}_{\mathrm{BSI}_{\mathrm{mod}}}^{\mathrm{TL}}(F,\omega,p)$, the effective potential barrier experienced by the electron is further reduced, resulting in a higher barrier-suppression ionization rate for both atoms. Consequently, the electron can escape more efficiently from the bound state, which leads to an enhanced ionization rate, see Fig. 4 (solid black line for helium atoms) and Fig. 5 (solid blue line for argon atoms). Previous experimental studies have verified the important role of the Coulomb interaction in strong-field ionization, both in the TI and BSI regimes [25], [26]. In particular, the long-range Coulomb potential has been shown to significantly influence measured photoelectron dynamics [26], while Coulomb-barrier-suppression models have been shown to reproduce experimentally observed enhanced ionization rates in the strong-field regime [25]. Moreover, the ionization rate $\mathrm{W}_{\mathrm{BSI}_{\mathrm{mod}}}^{\mathrm{TL}}(F,\omega,p)$ for argon is more sensitive to C_{corr}, Eq. (5), because argon enters the tunneling ionization regime at relatively lower laser intensities, see Fig. 4. In contrast, helium, owing to its higher ionization potential, is less sensitive to the influence of C_{corr} and requires stronger laser fields for comparable tunneling rates. Since helium enters the TI and BSI regimes at higher laser intensities, the effect of the long-range Coulomb

interaction on the ionization dynamics remains relatively weak, see Fig. 5. Our results show that the use of $W^{TL}_{BSI_{mod}}(F, \omega, p)$ improves the ionization rate predictions by approximately 10% for helium atoms and by nearly 25% for argon atoms. These quantitative differences demonstrate the magnitude of the improvement and highlight the enhanced accuracy of the proposed approach across the considered strong-field ionization regimes. These behaviors are consistent with the physical picture of strong-field ionization, in which the combined effects of the external laser field and the residual Coulomb potential determine the shape of the effective barrier and strongly influence electron dynamics and the ionization rate [15], [26], [27].

The results presented in this section demonstrate the validity and applicability of the analytical ionization rate models considered for linearly polarized laser fields. They also establish a reference framework for extending the analysis to other polarization states, where additional effects associated with electron dynamics and laser-field geometry become increasingly important.

CONCLUSION

The transition from the TI regime to the BSI regime has been systematically analyzed within an enhanced analytical framework that provides a more comprehensive description of strong-field ionization dynamics. The obtained results demonstrate that the ionization rate is influenced not only by the laser intensity but also by the initial momentum of the outgoing photoelectron and the laser frequency, highlighting the multidimensional nature of the ionization process, which is of particular importance in contemporary experiments. Furthermore, the analysis confirms that the long-range Coulomb interaction remains significant even in the BSI regime and cannot be neglected when accurately describing electron dynamics. While the strong laser field modifies the atomic potential and facilitates electron release, the residual Coulomb interaction governs important aspects of the electron motion after barrier suppression. Incorporating this contribution into the analytical model therefore improves the description of the ionization dynamics and provides more accurate ionization rate predictions across different parameters. These results help us better understand the connection between the TI and BSI regimes and provide a more reliable theoretical basis for modelling strong-field phenomena. Besides their essential importance, the results present novel avenues for investigating unexplored strong-field ionization mechanisms and improving our understanding of ultrafast laser-matter interactions.

ACKNOWLEDGEMENTS

Authors would like to acknowledge the support received from the Science Fund of the Republic of Serbia, #GRANT 6821, Atoms and (bio)molecules-dynamics and collisional processes on short time scale - ATMOLCOL. Our appreciation also goes to the Serbian Ministry of Education, Science and Technological Development (Agreement No. 451-03-34/2026-03/ 200122).

DECLARATIONS OF INTEREST STATEMENT

The authors affirm that there are no conflicts of interest to declare in relation to the research presented in this paper.

LITERATURE

1. L'Huillier, A. (2024). Nobel Lecture: The route to attosecond pulses. *Reviews of Modern Physics*, *96*, 030503. https://doi.org/10.1103/RevModPhys.96.030503
2. Krausz, F., & and Ivanov, M. (2009). Attosecond physics. *Reviews of Modern Physics*, *81*, 163–234. https://doi.org/10.1103/RevModPhys.81.163
3. L'Huillier, A., Lewenstein, M., P. Salières, P., & Balcou, P. (1993). High-order harmonic-generation processes in atoms in a strong laser field. *Physical Review A*, *48*, R3433. https://doi.org/10.1103/PhysRevA.48.R3433
4. Shvetsov-Shilovski, N. I. (2021). Semiclassical two-step model for ionization by a strong laser pulse: further developments and applications. *European Physical Journal D*, *75*, 130.

https://doi.org/10.1140/epjd/s10053-021-00134-3
5. Keldysh, L. V. (1965). Ionization in the field of a strong electromagnetic wave. *Soviet Physics JETP*, *20*, 1307–1314.
6. Ammosov, M. V., Delone, N. B., & Krainov, V. P. (1986). Tunnel ionization of complex atoms and atomic ions in an alternating electromagnetic field. *Soviet Physics JETP, 64*, 1191–1194.
7. Krainov, V. P. (1986). Ionization rates and energy and angular distributions at the barrier-suppression ionization of complex atoms and atomic ions. *Journal of the Optical Society of America B, 14*, 425–431. https://doi.org/10.1364/JOSAB.14.000425
8. Delone, N. B., & Krainov, V. P. (1985). *Atoms in Strong Light Fields*. Springer Series in Chemical Physics, Springer-Verlag.
9. Delone, N. B., & Krainov, V. P. (2000). *Multiphoton Processes in Atoms*. 2nd ed. Springer Series on Atomic, Optical, and Plasma Physics, Springer-Verlag. https://doi.org/10.1007/978-3-642-57208-1.
10. Krainov, V. P. (1998). Over-barrier ionization of atoms in strong laser fields. *Physics-Uspekhi*, *41*, 469–485.
11. Brabec, T., & Krausz, F. (2000). Intense few-cycle laser fields: Frontiers of nonlinear optics. *Reviews of Modern Physics*, *72*, 545–591. https://doi.org/10.1103/RevModPhys.72.545
12. Corkum, P. B. (1993). Plasma perspective on strong-field multiphoton ionization. *Physical Review Letters*, *71*, 1994–1997. https://doi.org/10.1103/PhysRevLett.71.1994
13. Tong, X. M., & Lin, C. D. (2005). Empirical formula for static field ionization rates of atoms and molecules by lasers in the barrier-suppression regime. *Journal of Physics B: Atomic, Molecular and Optical Physics*, *38*, 2593–2600. https://doi.org/10.1088/0953-4075/38/15/001
14. Krainov, V. P., & Ristić, V. M. (1992). Electron energy spectra in tunneling ionization of atoms and ions by a strong low-frequency electromagnetic field. *Soviet Physics JETP, 74*(5), 789–792.
15. Perelomov, A. M., Popov, V. S., & Terent'ev, M. V. (1966). Ionization of atoms in an alternating field. *Soviet Physics JETP*, *23*, 924.
16. D. Bauer, D. (2006). *Theory of intense laser-matter interaction*. Max-Planck Institute.
17. Petrović, V., Delibašić Marković, H., & Petrović, I. (2023). Coulomb corrected nonadiabatic instantaneous ionization rate and the electron trajectory in an elliptically polarized laser field. *Results in Physics*, *51*, 106718. https://doi.org/10.1016/j.rinp.2023.106718
18. Tong, X. M., Zhao, Z. X., & Lin, C. D. (2002). Theory of molecular tunneling ionization. *Physical Review A*, *66*, 033402. https://doi.org/10.1103/PhysRevA.66.033402
19. Becker, A., & Faisal, F. H. M. (2005). Intense-field many-body S-matrix theory. *Journal of Physics B*, *38*, R1–R56. https://doi.org/10.1088/0953-4075/38/3/R01
20. Corkum, P. B., & Krausz, F. (2007). Attosecond science. *Nature Physics*, *3*, 381–387. https://doi.org/10.1038/nphys620
21. Calvert, J. E., Palmer, A. J., Litvinyuk, I. V., & Sang, R. T. (2016). Metastable noble gas atoms in strong-field ionization experiments. *High Power Laser Science and Engineering*, *4*, e29. https://doi.org/10.1017/hpl.2016.32
22. Wallace, W. C. et al. (2016). Precise and accurate measurements of strong-field photoionization and a transferable laser intensity calibration standard. *Physical Review Letters*, *117*(5), 053001. https://doi.org/10.1103/PhysRevLett.117.053001
23. Shlomo, N., & Frumker, E. (2025). In situ characterization of laser-induced strong field ionization phenomena. *Light: Science & Applications*, *14*, 166. https://doi.org/10.1038/s41377-025-01808-y
24. Popruzhenko, S. V., Mur, V. D., Popov, V. S., & Bauer, D. (2008). Strong Field Ionization Rate for Arbitrary Laser Frequencies. *Physical Review Letters*,*101*, 193003. https://doi.org/10.1103/PhysRevLett.101.193003
25. Augst, S., Meyerhofer, D. D., Strickland, D., & Chin, S. L. (1991). Laser ionization of noble gases by Coulomb-barrier suppression. *Journal of the Optical Society of America B*, *8*, 858-867. https://doi.org/10.1364/JOSAB.8.000858

26. Quan, W., Hao, X., Chen, Y. *et al.* (2016). Long-Range Coulomb Effect in Intense Laser-Driven Photoelectron Dynamics. *Scientific Reports*, *6*, 27108. https://doi.org/10.1038/srep27108
27. Becker, W., Liu, X., Ho, P. J., & Eberly, J. H. (2012). Theories of photoelectron correlation in strong-field laser physics. *Reviews of Modern Physics*, *84*, 1011. https://doi.org/10.1103/RevModPhys.84.1011